Time evolution of entangled Bell states in coupled quantum dots in the presence of fluctuations

N. S. Maslova,[1] V. N. Mantsevich,[2] I. M. Sokolov,[3] and P. I. Arseyev[4]

[1]*Chair of Quantum electronics, Physics Department, Lomonosov Moscow State University, 119991 Moscow, Russia*

[2]*Chair of Semiconductors and Cryoelectronics, Physics Department, Lomonosov Moscow State University, 119991 Moscow, Russia*

[3]*Institut für Physik and IRIS Adlershof, Humboldt University Berlin, Newtonstrasse 15, 12489 Berlin, Germany*

[4]*P.N. Lebedev Physical Institute RAS, 119991 Moscow, Russia*

(Received 22 November 2023; accepted 6 March 2024; published 25 March 2024)

We analyze the dynamics of two-qubit entangled Bell states in coupled quantum dots (QDs) in the presence of both fluctuations and coherent electron hopping between the dots. The explicit expression for time-dependent probability to find the system in the different Bell states was obtained for various initial conditions by means of Keldysh diagram technique. It was revealed that time evolution of one pair of Bell states and its decay rate strongly differs from another one. It was demonstrated that one pair of Bell states is more robust against fluctuations than another one. The stationary occupation of Bell states for different initial conditions was also analyzed. Obtained results are important for the problems where long-living Bell states are needed such as the security of quantum communication and quantum information processing.

DOI: 10.1103/PhysRevA.109.032430

I. INTRODUCTION

Semiconductor quantum dots (QDs) are promising objects for the scalable quantum information processing using the localized electrons and spins as qubits [1,2]. So, among the most important problems in the present-day solid-state physics is the controllable formation, manipulation, and read out of entangled states [3–7]. Entangled states open the possibility to organize safe dense coding [8], secure quantum communication [9], quantum key distribution [10], and quantum teleportation [11]. Coupled QDs seem to be very perspective for single- and two-electronic states initialization, processing, and read out with high accuracy [12–19]. Experimentally, entangled states in correlated QDs can be controlled by external gate voltage [20,21] or by external laser pulses [22,23]. Recent experiments also demonstrate that spin system of a semiconductor QD is a promising platform for long-distance quantum communications [24–27]. However, kinetics of charge and spin states in QDs is strongly affected by fluctuations caused by electron-phonon interaction, fluctuation of external field, and Coulomb correlations [28–41]. It should be noted that interaction with environment is extremely important for quantum computation as it strongly influences the dynamics and stability of entangled states.

Single- and two-qubit states are affected by both environmental fluctuations and fluctuations within the system caused by the presence of interparticle interaction. As a result, the presence of noise often reduces the probability to find the system in its initial entangled state. Moreover, noise usually reduces qubit's readout [42–44]. Experimental investigations of QDs systems demonstrated rather strong noise even at low cryogenic temperatures [45–48]. The fluctuations can be caused by classical stochastic processes as well as by quantum effects [49–52]. For example, in real systems noise can be caused by electron-phonon interaction or by the presence of the external field fluctuations. Noise correlation functions can be quite different varying from the white noise (δ correlated) to the power-law decreasing correlations.

In the present paper the stability of single- and entangled two-qubit states in the coupled QD is analyzed theoretically. We consider the situation when QD's energy levels fluctuate due to the interaction with the environment. Direct calculations of time-dependent probability to find the system in its initial state are presented. It was found that the decay law considerably differs for various types of initial Bell states.

II. THEORETICAL MODEL AND MAIN RESULTS

A. Model of the system

We consider two coupled single-level QDs with independently fluctuating energy levels and coherent hopping of electrons between them. Spin-up σ and spin-down $-\sigma$ electrons could be localized in each QD. Such model describes two-qubit system affected by noise. The Hamiltonian of the system reads

$$\hat{H} = \sum_{\sigma}[T(\hat{c}_{1\sigma}^{\dagger}\hat{c}_{2\sigma} + \hat{c}_{2\sigma}^{\dagger}\hat{c}_{1\sigma}) + \xi_1(t)\hat{c}_{1\sigma}^{\dagger}\hat{c}_{1\sigma} + \xi_2(t)\hat{c}_{2\sigma}^{\dagger}\hat{c}_{2\sigma}], \tag{1}$$

where operator $\hat{c}_{1(2)\sigma}^{\dagger}$ corresponds to the electron creation in the first (second) QD. Coherent transitions are described by amplitude T and $\xi_i(t)$ corresponds to the presence of white noise caused by fluctuations of energy levels 1 and 2 in QDs with correlation function $\langle\xi_{1(2)}(t)\xi_{1(2)}(t')\rangle = Q\delta(t-t')$ and $\langle\xi_{1(2)}(t)\xi_{2(1)}(t')\rangle = 0$.

At the initial time moment different types of Bell states can be prepared in the QDs. Further we will analyze two types of Bell states:

$$|\Psi_{\pm}(0)\rangle = \frac{|1\rangle_{\sigma}|2\rangle_{-\sigma} \pm |1\rangle_{-\sigma}|2\rangle_{\sigma}}{\sqrt{2}},$$
$$|\Phi_{\pm}(0)\rangle = \frac{|1\rangle_{\sigma}|1\rangle_{-\sigma} \pm |2\rangle_{\sigma}|2\rangle_{-\sigma}}{\sqrt{2}}. \tag{2}$$

Modern technology allows to form electrically induced coupled QDs by means of electrostatic gates, which precisely control energy levels, heights of tunnel barriers, and the strength of exchange interaction [24–27]. Initial states $|\Psi_{\pm}(0)\rangle$ can be prepared for deep energy levels by means of adiabatic switching of exchange interaction, varying both detuning between the QDs energy levels and tunnel-barriers height. Such procedure allows to form singlet state $|\Psi_{-}(0)\rangle$. Triplet state $|\Psi_{+}(0)\rangle$ can be obtained from the singlet state $|\Psi_{-}(0)\rangle$ by a $\pi/2$ pulse of a gradient magnetic field B_z applied between the dots.

Initial states $|\Phi_{\pm}(0)\rangle$ can be obtained from the state with two electrons localized in one of the QDs in the absence of coupling between them. Applying gate voltage the barrier height between the dots could be decreased. So, one can get the strong hopping regime, when coherent hopping amplitude significantly exceeds the noise amplitude. Switching off coherent electron transitions between QDs during the time interval $\tau_0 = \pi/4 \cdot T$ with a particularly chosen phase results in the formation of $|\Phi_{\pm}(0)\rangle$ states. Further, the barrier height should be increased adiabatically, driving the system to the state $|\Phi_{\pm}(0)\rangle$, corresponding to small coherent hopping and strongly fluctuating energy levels.

B. Time evolution of a single-qubit state

Let us first consider time evolution of a single-qubit state. Further, for simplicity we will omit index σ. If at the initial time moment the electron is localized in the QD 1, the initial-state wave function reads $|\psi(0)\rangle = |1\rangle$ (in the second quantization representation the initial state reads $|1\rangle = c_1^{\dagger}|vac\rangle$). The probabilities P_{11} and P_{12} to find an electron during time evolution in QD 1 or in QD 2 can be written in the second quantization representation

$$P_{11(12)} = \langle\langle\hat{c}_{1\sigma}(t)\hat{c}^{\dagger}_{1(2)\sigma}(0)\rangle\langle\hat{c}_{1(2)\sigma}(0)\hat{c}^{\dagger}_{1\sigma}(t)\rangle\rangle_{\xi}. \tag{3}$$

Using Green-functions formalism one can rewrite Eq. (3) in the following form

$$\begin{aligned} P_{11} &= \langle G^{>}_{11}(t,0)G^{>}_{11}(0,t)\rangle_{\xi} \\ &= \int d\omega \int \frac{d\Omega}{2\pi}\big\langle G^{R}_{11}(\Omega+\omega)G^{A}_{11}\Omega)\big\rangle_{\xi} e^{-i\omega t}, \\ P_{21} &= \langle G^{>}_{21}(t,0)G^{>}_{12}(0,t)\rangle_{\xi} \\ &= \int d\omega \int \frac{d\Omega}{2\pi}\big\langle G^{R}_{21}(\Omega+\omega)G^{A}_{12}\Omega)\big\rangle_{\xi} e^{-i\omega t}. \end{aligned} \tag{4}$$

The presence of white noise leads to the appearance of only diagonal self-energy parts $\Sigma^{R(A)}_{ii}$ in the averaged Green functions in zero order in T. The diagrams contributing to the self-energy parts are shown in Fig. 1.

$$\begin{aligned} \Sigma^{R(A)}_{ii}(t,t') &= \mp iQ\delta(t-t'), \\ \Sigma^{R(A)}_{ij}(t,t') &= 0. \end{aligned} \tag{5}$$

Diagrams with crossing-noise correlation functions vanish for the white noise. So, white noise results only in Ω renormalization, i.e., $\Omega \to \Omega \pm iQ$.

$$\big\langle G^{0R(A)}_{ii}(\Omega)\big\rangle_{\xi} = \frac{1}{\Omega \pm iQ}. \tag{6}$$

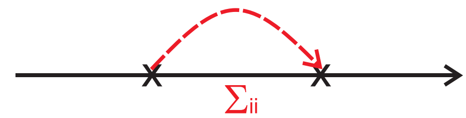

FIG. 1. Diagrams contributing to the zero order in T Green functions $\langle G^{0R(A)}_{ii}(\Omega)\rangle_{\xi}$.

Retarded and advanced Green functions were obtained in a usual way from Dyson equations, considering the first (hopping) term in the Hamiltonian Eq. (1) as a perturbation. Zero-order Green functions are determined by Eq. (6). So, one can get the following expressions for $\langle G^{R(A)}_{11}(\Omega)\rangle_{\xi}$ and $\langle G^{R(A)}_{12}(\Omega)\rangle_{\xi}$:

$$\begin{aligned} \big\langle G^{R(A)}_{11}(\Omega)\big\rangle_{\xi} &= \big\langle G^{R(A)}_{22}(\Omega)\big\rangle_{\xi} = \frac{\Omega \pm iQ}{(\Omega \pm iQ)^2 - T^2}, \\ \big\langle G^{R(A)}_{12}(\Omega)\big\rangle_{\xi} &= \big\langle G^{R(A)}_{21}(\Omega)\big\rangle_{\xi} = \frac{T}{(\Omega \pm iQ)^2 - T^2}. \end{aligned} \tag{7}$$

Further we omit index ξ and averaging over ξ is included in the angle-brackets symbol $\langle\rangle_{\xi} \equiv \langle\rangle$. To get an expression for P_{11} one should calculate

$$\begin{aligned} \int d\Omega\big\langle G^{R}_{11(22)}(\Omega+\omega)G^{A}_{11(22)}(\Omega)\big\rangle &= K_{11}\Pi_{11} + K_{12}\Pi_{21} \\ &= \frac{1}{2}(KX + \bar{K}Y), \end{aligned} \tag{8}$$

where $K = K_{11} + K_{12}$, $\bar{K} = K_{11} - K_{12}$ and $X = \Pi_{11} + \Pi_{21}$, $Y = \Pi_{11} - \Pi_{21}$ with

$$K_{11(12)} = \int \frac{d\Omega}{2\pi}\big\langle G^{R}_{11(12)}(\Omega+\omega)\big\rangle\big\langle G^{A}_{11(12)}(\Omega)\big\rangle. \tag{9}$$

Exact expressions for K_{11} and K_{12} read

$$\begin{aligned} K_{11} &= \frac{(\omega+2iQ)^2 - 2T^2}{(\omega+2iQ)[(\omega+2iQ)^2 - 4T^2]} = K_{22}, \\ K_{12} &= \frac{-2T^2}{(\omega+2iQ)[(\omega+2iQ)^2 - 4T^2]} = K_{21}. \end{aligned} \tag{10}$$

Polarization operators Π_{11} and Π_{21} for white noise are determined by the ladder diagrams shown in Fig. 2. Thus, polarization operators satisfy the following equations:

$$\begin{aligned} \Pi_{11} &= 1 + 2iQK_{11}\Pi_{11} + 2iQK_{12}\Pi_{21}, \\ \Pi_{21} &= 1 + 2iQK_{22}\Pi_{21} + 2iQK_{21}\Pi_{11}. \end{aligned} \tag{11}$$

These equations can be rewritten in X and Y terms in the following way:

$$\begin{aligned} X &= 1 + 2iQKX, \\ Y &= 1 + 2iQ\bar{K}Y. \end{aligned} \tag{12}$$

Using equations for K_{11} and K_{12} one can get K and $\bar{K}$:

$$\begin{aligned} K &= \frac{1}{\omega + 2iQ}, \\ \bar{K} &= \frac{(\omega+2iQ)}{(\omega+2iQ)^2 - 4T^2}. \end{aligned} \tag{13}$$

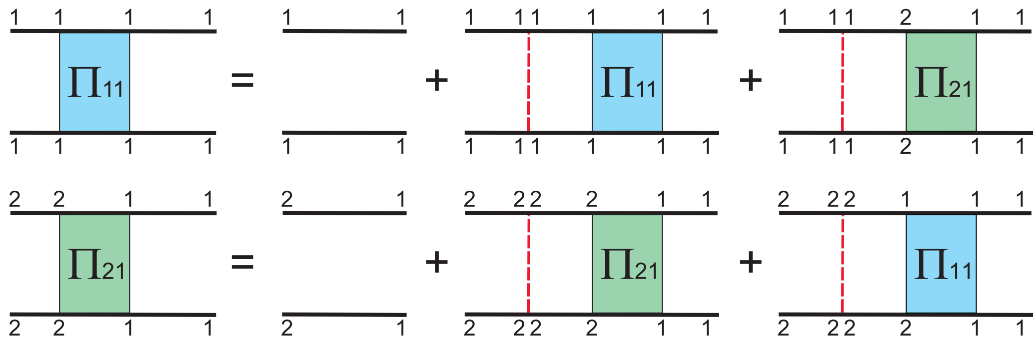

FIG. 2. Ladder diagrams contributing to the polarization operators Π_{ij}.

So, explicit expressions for X and Y read

$$X = \frac{\omega + 2iQ}{\omega},$$
$$Y = \frac{(\omega + 2iQ)^2 - 4T^2}{\omega(\omega + 2iQ) - 4T^2}. \tag{14}$$

Let us further consider the following notation

$$\int d\Omega \langle G^R_{ij}(\Omega + \omega) G^A_{kl}(\Omega)\rangle \equiv \langle G^R_{ij} G^A_{kl}\rangle_\omega. \tag{15}$$

To get the probability time evolution to find an electron in the QD 1, one should calculate an expression

$$P_{11}(t) = \int \frac{d\omega}{2\pi} \langle G^R_{11} G^A_{11}\rangle_\omega e^{-i\omega t}. \tag{16}$$

Using expressions for K, $\bar{K}$, X, and Y one can get a direct expression for $\langle G^R_{11} G^A_{11}\rangle_\omega$:

$$\langle G^R_{11} G^A_{11}\rangle_\omega = \frac{1}{2}(KX + \bar{K}Y)$$
$$= \frac{1}{2}\left(\frac{1}{\omega} + \frac{\omega + 2iQ}{\omega(\omega + 2iQ) - 4T^2}\right). \tag{17}$$

Analogously, the probability time evolution to find an electron in the QD 2 can be written as

$$P_{21}(t) = \int \frac{d\omega}{2\pi} \langle G^R_{12} G^A_{21}\rangle_\omega e^{-i\omega t}, \tag{18}$$

with

$$\langle G^R_{12} G^A_{21}\rangle_\omega = \frac{1}{2}(KX - \bar{K}Y)$$
$$= \frac{1}{2}\left(\frac{1}{\omega} - \frac{\omega + 2iQ}{\omega(\omega + 2iQ) - 4T^2}\right). \tag{19}$$

From Eqs. (16)–(19) one can get the time-dependent probability to find the system in the same initial state P_{11} and the probability to find the system in the state 2 (P_{21}), if it was initially in the state 1:

$$P_{11}(t) = \frac{1}{2} + \frac{1}{2}\left[\left(1 + \frac{T^2}{Q^2}\right)e^{-\frac{2T^2 t}{Q}} - \frac{T^2}{Q^2}e^{-2Qt}\right] = \frac{1+x}{2},$$
$$P_{21}(t) = \frac{1}{2} - \frac{1}{2}\left[\left(1 + \frac{T^2}{Q^2}\right)e^{-\frac{2T^2 t}{Q}} - \frac{T^2}{Q^2}e^{-2Qt}\right] = \frac{1-x}{2}. \tag{20}$$

Solid and dashed black curves in Fig. 3 demonstrate the probability time evolution for a single qubit state to find the system in the state 1 or 2 if it was initially in the state 1 in the presence of noise. For the initial state $|s(a)\rangle = \frac{|1\rangle \pm |2\rangle}{\sqrt{2}}$ the probability to find the system in its initial state $s(a)$ is defined similar to Eq. (3) by substituting $1 \leftrightarrow s$ and $2 \leftrightarrow a$. Taking into account relation $c_{s(a)\sigma} = \frac{c_{1\sigma} \pm c_{2\sigma}}{\sqrt{2}}$ and using second quantization representation one can find by means of Keldysh diagram technique

$$P_{ss}(t) = \frac{1}{4}\langle (G^>_{11}(t,0) + G^>_{22}(t,0) + G^>_{21}(t,0) + G^>_{12}(t,0))$$
$$\times (G^>_{11}(0,t) + G^>_{22}(0,t) + G^>_{21}(0,t) + G^>_{12}(0,t))\rangle. \tag{21}$$

From expressions (7) one can directly get

$$\int d\Omega [\langle G^R_{11}(\Omega)\rangle \langle G^A_{12}(\Omega + \omega)\rangle$$
$$+ \langle G^R_{12}(\Omega)\rangle \langle G^A_{11}(\Omega + \omega)\rangle] = 0. \tag{22}$$

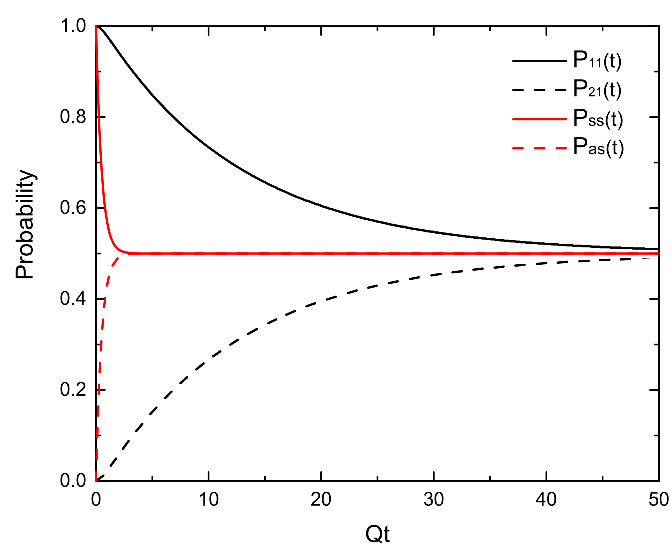

FIG. 3. Probability to find the system in the state 1 (s) or 2 (a) if it was initially in the state 1 (s) [$P_{11(ss)}(t)$ and $P_{21(as)}(t)$ correspondingly] in the presence of noise. Solid and dashed black curves are obtained over Eq. (20), solid and dashed red curves are obtained over Eq. (29). Parameter $T = 0.2Q$ is equal for all the curves.

Thus the Fourier amplitude of $P_{ss}(t)$ can be written as

$$\begin{aligned} P_{ss}(\omega) = {} & \tfrac{1}{4}\big[\big\langle G_{11}^R G_{11}^A\big\rangle_\omega + \big\langle G_{22}^R G_{22}^A\big\rangle_\omega \\ & + \big\langle G_{12}^R G_{21}^A\big\rangle_\omega + \langle G_{21}^R G_{21}^A\rangle_\omega\big] \\ & + \tfrac{1}{4}\big[\big\langle G_{11}^R G_{22}^A\big\rangle_\omega + \big\langle G_{22}^R G_{11}^A\big\rangle_\omega \\ & + \big\langle G_{12}^R G_{12}^A\big\rangle_\omega + \big\langle G_{21}^R G_{21}^A\big\rangle_\omega\big]. \end{aligned} \tag{23}$$

From Eqs. (17)–(19) one can obtain

$$\frac{1}{4}\big[\big\langle G_{11}^R G_{11}^A\big\rangle_\omega + \big\langle G_{22}^R G_{22}^A\big\rangle_\omega + \big\langle G_{12}^R G_{21}^A\big\rangle_\omega + \big\langle G_{21}^R G_{21}^A\big\rangle_\omega\big] = \frac{1}{2\omega}. \tag{24}$$

Fourier transform of Eq. (24) has the form

$$\begin{aligned} \frac{1}{4}\int & \big[\big\langle G_{11}^R G_{11}^A\big\rangle_\omega + \big\langle G_{22}^R G_{22}^A\big\rangle_\omega \\ & + \big\langle G_{12}^R G_{21}^A\big\rangle_\omega + \big\langle G_{21}^R G_{21}^A\big\rangle_\omega\big] e^{i\omega t}dt = \frac{1}{2}. \end{aligned} \tag{25}$$

As $\langle \xi_1(t)\xi_2(t')\rangle = 0$ ladder diagrams do not appear for the correlation function $\langle G_{11}^R G_{22}^A\rangle_\omega$, so

$$\begin{aligned} \big\langle G_{11}^R G_{22}^A\big\rangle_\omega &= \int d\Omega \big\langle G_{11}^R(\Omega+\omega)\big\rangle \big\langle G_{22}^A(\Omega)\big\rangle \\ &= \frac{(\omega+2iQ)^2 - 2T^2}{(\omega+2iQ)[(\omega+2iQ)^2 - 4T^2]}. \end{aligned} \tag{26}$$

Analogously,

$$\begin{aligned} \big\langle G_{12}^R G_{12}^A\big\rangle_\omega &= \int d\Omega \big\langle G_{12}^R(\Omega+\omega)\big\rangle \big\langle G_{12}^A(\Omega)\big\rangle \\ &= \frac{-2T^2}{(\omega+2iQ)[(\omega+2iQ)^2 - 4T^2]}. \end{aligned} \tag{27}$$

From Eqs. (26)–(27) one can easily get

$$\begin{aligned} \frac{1}{4}\int & \big[\big\langle G_{11}^R G_{22}^A\big\rangle_\omega + \big\langle G_{22}^R G_{11}^A\big\rangle_\omega + \big\langle G_{12}^R G_{12}^A\big\rangle_\omega \\ & + \big\langle G_{21}^R G_{21}^A\big\rangle_\omega\big] e^{-i\omega t}d\omega = \frac{1}{2}e^{-2Qt}. \end{aligned} \tag{28}$$

Finally,

$$P_{ss(as)}(t) = \frac{1 \pm e^{-2Qt}}{2}. \tag{29}$$

Solid and dashed red curves in Fig. 3 demonstrate the probability time evolution for a single qubit state to find the system in the state s or a if it was initially in the state s in the presence of noise.

C. Time evolution of a two-qubit state

Let us define two-qubit initial state $|1\rangle_\sigma|2\rangle_{-\sigma}$ when electron with spin σ is localized in the first QD $|1\rangle$ and electron with spin $-\sigma$ is localized in the second QD $|2\rangle$. We consider initial state as a superposition of state $|1\rangle_\sigma|2\rangle_{-\sigma}$ and the "opposite" state when electron with spin $-\sigma$ is localized in the first QD $|1\rangle$ and electron with spin σ is localized in the second QD $|2\rangle$: $|1\rangle_{-\sigma}|2\rangle_\sigma$. The corresponding wave function reads

$$|\Psi_\pm(0)\rangle = \frac{|1\rangle_\sigma|2\rangle_{-\sigma} \pm |1\rangle_{-\sigma}|2\rangle_\sigma}{\sqrt{2}}. \tag{30}$$

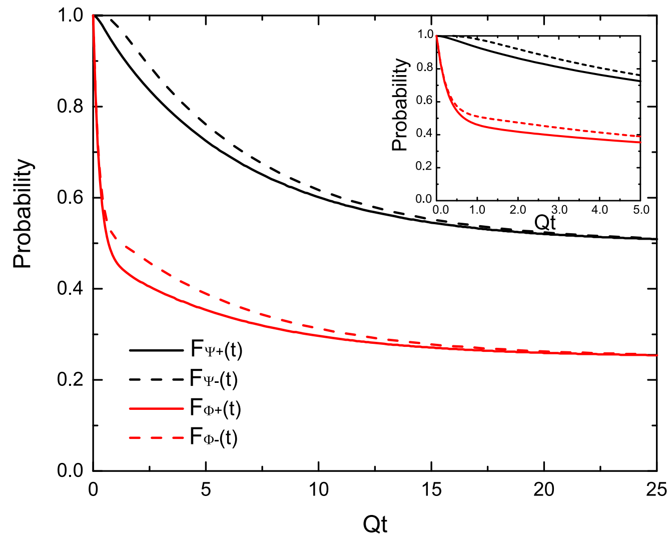

FIG. 4. Probability time evolution for a two-qubit state to find the system in its initial state in the presence of noise. Solid and dashed black curves are obtained over Eq. (32), solid and dashed red curves are obtained over Eq. (36). The insert shows zoomed fidelity time evolution at the initial stage. $T = 0.2Q$.

Further we will use the designation $\sigma \to +$ and $-\sigma \to -$. In the second quantization representation the probability to find the system in the initial state $|\Psi_\pm(0)\rangle$ during time evolution can be expressed as

$$\begin{aligned} F_{\Psi_\pm}(t) &= \langle |\langle \Psi_\pm(0)|\Psi_\pm(t)\rangle|^2\rangle \\ &= \frac{1}{4}\langle (G_{11}^{>++}(t,0)G_{22}^{>--}(t,0) + G_{11}^{>--}(t,0)G_{22}^{>++}(t,0) \\ &\quad \pm G_{12}^{>++}(t,0)G_{21}^{>--}(t,0) \pm G_{21}^{>++}(t,0)G_{12}^{>--}(t,0)) \\ &\quad \times (G_{11}^{>++}(0,t)G_{22}^{>--}(0,t) + G_{11}^{>--}(0,t)G_{22}^{>++}(0,t) \\ &\quad \pm G_{12}^{>++}(0,t)G_{21}^{>--}(0,t) \\ &\quad \pm G_{21}^{>++}(0,t)G_{12}^{>--}(0,t))\rangle. \end{aligned} \tag{31}$$

The details of function $F_{\Psi_\pm}(t)$ calculation are presented in Appendix A. An expression for $F_{\Psi_\pm}(t)$ has a rather simple form

$$F_{\Psi_\pm} = \frac{1+x^2(t)}{2} \mp \frac{T^2}{Q^2}\big[e^{-\frac{2T^2 t}{Q}} - e^{-2Qt}\big]^2, \tag{32}$$

where $x(t) = (1 + \frac{T^2}{Q^2})e^{-\frac{2T^2 t}{Q}} - \frac{T^2}{Q^2}e^{-2Qt}$ (see Appendix A). For $T \ll Q$ expression (32) can be written up to the terms proportional to T^2/Q^2 as

$$F_{\Psi_\pm} = \frac{1 + e^{\frac{-4T^2 t}{Q}}}{2}. \tag{33}$$

Solid and dashed black curves in Fig. 4 demonstrate the probability time evolution for a two-qubit state to find the system in its initial state $F_{\Psi_\pm}$ in the presence of noise. Another possible two-qubit initial state deals with the situation when two electrons with opposite spins are localized in the same quantum dot—the first one $|1\rangle$ or the second one $|2\rangle$—so the initial state is a quantum superposition of the states $|1\rangle_\sigma|1\rangle_{-\sigma}$

and $|2\rangle_\sigma|2\rangle_{-\sigma}$. Corresponding wave function reads

$$|\Phi_\pm(0)\rangle = \frac{|1\rangle_\sigma|1\rangle_{-\sigma} \pm |2\rangle_\sigma|2\rangle_{-\sigma}}{\sqrt{2}}. \quad (34)$$

Following the logic of the previously analyzed case, one can write down an expression for $F_{\Phi_\pm}$:

$$\begin{aligned} F_{\Phi_\pm} = \tfrac{1}{4}\langle (&G_{11}^{>++}(t,0)G_{11}^{>--}(t,0) + G_{22}^{>++}(t,0)G_{22}^{>--}(t,0) \\ &\pm G_{12}^{>++}(t,0)G_{12}^{>--}(t,0) \pm G_{21}^{>++}(t,0)G_{21}^{>--}(t,0)) \\ &\times (G_{11}^{>++}(0,t)G_{11}^{>--}(0,t) + G_{22}^{>++}(0,t)G_{22}^{>--}(0,t) \\ &\pm G_{12}^{>++}(0,t)G_{12}^{>--}(0,t) \pm G_{21}^{>++}(0,t)G_{21}^{>--}(0,t))\rangle. \end{aligned} \quad (35)$$

The detailed calculations of function $F_{\Phi_\pm}$ are presented in Appendix B. An expression for $F_{\Phi_\pm}(t)$ reads

$$\begin{aligned} F_{\Phi_\pm} &= \frac{1+x^2(t)}{4} + \frac{1+cos^2(2Tt)}{4}e^{-4Qt} \\ &\pm \frac{T^2}{Q^2}[e^{-\frac{2T^2t}{Q}} - e^{-2Qt}]^2. \end{aligned} \quad (36)$$

For $T \ll Q$ oscillations are not present as the last term is of the order of T^2/Q^2 and considering terms up to T^2/Q^2 expression (36) can be rewritten in the form

$$F_{\Phi_\pm} = \frac{1+e^{\frac{-4T^2t}{Q}}}{4} + \frac{1}{2}e^{-4Qt}. \quad (37)$$

Solid and dashed red curves in Fig. 4 demonstrate the probability time evolution for a two-qubit state to find the system in its initial state $F_{\Phi_\pm}$ in the presence of noise.

D. Experimental initialization of qubit states

Finally, we should discuss the possibility of two-qubit states preparation in a double QD available experimentally nowadays. Experimental techniques are typically based on rapid electrical control of the exchange interaction [53,54]. The qubits preparation usually starts from the states $|1\rangle_\sigma|1\rangle_{-\sigma}$ or $|2\rangle_\sigma|2\rangle_{-\sigma}$, which can be initialized by means of the tunnel-barrier parameters tuning between the dot and the reservoir (coupling between the dots is switched off), so QD becomes sequentially occupied by a single electron and then by two electrons with opposite spins due to the Pauli principle. Switching on interaction between the dots allows to drive the system from the state $|1(2)\rangle_\sigma|1(2)\rangle_{-\sigma}$ to the state $|1\rangle_\sigma|2\rangle_{-\sigma}$. Once initializing the system in the $|1\rangle_\sigma|2\rangle_{-\sigma}$ state, the application of a finite exchange J for a time τ rotates the spin state about z axis of the Bloch sphere, in the plane containing both $|1\rangle_\sigma|2\rangle_{-\sigma}$ and $|1\rangle_{-\sigma}|2\rangle_\sigma$ states, so one can perform a SWAP operation, rotating the state $|1\rangle_\sigma|2\rangle_{-\sigma}$ into the state $|1\rangle_{-\sigma}|2\rangle_\sigma$ [53]. In Ref. [54] the following transitions were observed: $|1\rangle_{-\sigma}|2\rangle_\sigma \to |1\rangle_\sigma|2\rangle_\sigma$ and $|1\rangle_\sigma|2\rangle_{-\sigma} \to |1\rangle_{-\sigma}|2\rangle_{-\sigma}$, using electrical pulses that control the exchange coupling between the qubits. An alternative mechanism deals with the use of nonuniform magnetic or oscillating magnetic fields leading to the conditions when electron spin resonance arises to manipulate spins [55]. In this case starting from the $|1\rangle_\sigma|2\rangle_\sigma$ state, the electron spin resonance with the left (right) electron changes the initial state to the $|1\rangle_\sigma|2\rangle_{-\sigma}$ or $|1\rangle_{-\sigma}|2\rangle_\sigma$ configuration [55]. In Ref. [56] authors demonstrated the initialization of a long-lived single-electron spin qubit in a Si/SiGe QD with all-electrical two-axis control. The spin was driven by resonant microwave electric fields in a transverse magnetic-field gradient from a local micromagnet. The step by step description of double QDs system initialization in the single-qubit state and in the two-qubit state $|1\rangle_{-\sigma}|2\rangle_{-\sigma}$ by "shaking" the electron spins in the transverse field gradient of the micromagnet is presented in Ref. [57]. The CNOT gate was used to create the Bell state $|\psi\rangle = \frac{1}{\sqrt{2}}(|1\rangle_{-\sigma}|2\rangle_{-\sigma} - i|1\rangle_\sigma|2\rangle_\sigma)$ after initialization of the state $|1\rangle_\sigma|2\rangle_{-\sigma}$ and $|1\rangle_{-\sigma}|2\rangle_\sigma$ and performing transitions to the states $|1\rangle_\sigma|2\rangle_\sigma$ and $|1\rangle_{-\sigma}|2\rangle_{-\sigma}$, correspondingly, using long direct-current exchange pulse and varying the length of microwave pulse, which adiabatically flips one of the spins. Finally, in Ref. [58] the initialization and quantum-state tomography of Bell states $\frac{|1\rangle_\sigma|2\rangle_\sigma \pm |1\rangle_{-\sigma}|2\rangle_{-\sigma}}{\sqrt{2}}$ and $\frac{|1\rangle_\sigma|2\rangle_{-\sigma} \pm |1\rangle_{-\sigma}|2\rangle_\sigma}{\sqrt{2}}$ was performed. The measured fidelities of each Bell state were found to be $87.1 \pm 2.8\%$, $90.3 \pm 3.0\%$, $90.3 \pm 2.4\%$, and $90.2 \pm 2.9\%$. So, states $|\Psi_\pm\rangle$ and states $|1(2)\rangle_\sigma|1(2)\rangle_{-\sigma}$ are well achievable experimentally. To get the state $|\Phi_\pm\rangle$, one should initialize the states $|1\rangle_\sigma|2\rangle_{-\sigma}$ and $|2\rangle_\sigma|1\rangle_{-\sigma}$ and then excite the system by means of microwave pulses. For the wavelength exceeding the system size and rather large energy relaxation times, the system will be in excited $|\Phi_\pm\rangle$ state.

III. CONCLUSIONS

We performed detailed analysis of the two-qubit entangled Bell-states stability in coupled QDs in the presence of fluctuations. The presence of white noise allowed to solve the problem exactly by means of Keldysh diagram technique. The considered model revealed that various types of initial entangled Bell states demonstrate different robustness against noise. Moreover, time evolution of two pairs of Bell states differs strongly. Obtained results are useful for the problems where long-living Bell states could be applied, for example the security of quantum communication and quantum information processing.

ACKNOWLEDGMENTS

V.N.M. thanks the Foundation for the Advancement of Theoretical Physics and Mathematics "BASIS."

APPENDIX A: TIME EVOLUTION OF TWO-QUBIT STATE $F_{\Psi_\pm}$

Let us obtain an expression for probability $F_{\Psi_\pm}$ for the Bell states

$$|\Psi_\pm(0)\rangle = \frac{|1\rangle_\sigma|2\rangle_{-\sigma} \pm |1\rangle_{-\sigma}|2\rangle_\sigma}{\sqrt{2}}. \quad (A1)$$

Let us calculate all the contributions to expression (31). Taking into account Eq. (17) one can get

$$\begin{aligned} &\frac{1}{4}\langle G_{11}^{>++}(t,0)G_{22}^{>--}(t,0) + G_{11}^{>--}(t,0)G_{22}^{>++}(t,0) \\ &\quad \times |G_{11}^{>++}(0,t)G_{22}^{>--}(0,t) + G_{11}^{>--}(0,t)G_{22}^{>++}(0,t)\rangle \end{aligned}$$

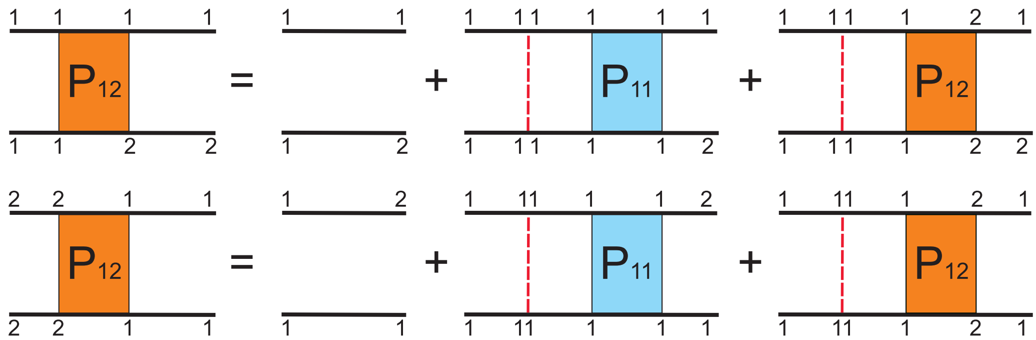

FIG. 5. Ladder diagrams contributing to the polarization operators Π_{ij}.

$$\begin{aligned}
&= \frac{1}{4}4\int d\omega_1 d\omega_2 \langle G^R_{11}G^A_{11}\rangle_{\omega_1}\langle G^R_{22}G^A_{22}\rangle_{\omega_2} e^{-i\omega_1 t}e^{-i\omega_2 t}\\
&= \frac{1}{4}(1+x(t))^2, \qquad \text{(A2)}
\end{aligned}$$

where $x(t) = (1+\frac{T^2}{Q^2})e^{-\frac{2T^2 t}{Q}} - \frac{T^2}{Q^2}e^{-2Qt}$. Analogously, considering Eq. (19) one can find

$$\begin{aligned}
&\frac{1}{4}\langle G^{>++}_{21}(t,0)G^{>--}_{12}(t,0) + G^{>--}_{21}(t,0)G^{>++}_{12}(t,0)\\
&\quad\times |G^{>++}_{21}(0,t)G^{>--}_{12}(0,t) + G^{>--}_{21}(0,t)G^{>++}_{12}(0,t)\rangle\\
&= \frac{1}{4}4\int d\omega_1 d\omega_2 \langle G^R_{12}G^A_{21}\rangle_{\omega_1}\langle G^R_{21}G^A_{12}\rangle_{\omega_2} e^{-i\omega_1 t}e^{-i\omega_2 t}\\
&= \frac{1}{4}(1-x(t))^2. \qquad \text{(A3)}
\end{aligned}$$

Let us analyze the remaining terms

$$\begin{aligned}
R = {}& \tfrac{1}{4}\langle (G^{>++}_{22}(t,0)G^{>--}_{11}(t,0) + G^{>--}_{22}(t,0)G^{>++}_{11}(t,0))\\
&\times (G^{>++}_{12}(0,t)G^{>--}_{21}(0,t) + G^{>--}_{12}(0,t)G^{>++}_{21}(0,t))\rangle\\
&+ \frac{1}{4}\langle (G^{>++}_{12}(t,0)G^{>--}_{21}(t,0) + G^{>--}_{21}(t,0)G^{>++}_{12}(t,0))\\
&\times (G^{>++}_{22}(0,t)G^{>--}_{11}(0,t) + G^{>--}_{11}(0,t)G^{>++}_{22}(0,t))\rangle. \qquad \text{(A4)}
\end{aligned}$$

Let us consider the following averaged combination of Green's functions denoted as H:

$$\begin{aligned}
H = {}& \langle G^{>++}_{11}(t,0)G^{>++}_{21}(0,t)G^{>--}_{22}(t,0)G^{>--}_{12}(0,t)\\
&+ G^{>++}_{21}(t,0)G^{>++}_{11}(0,t)G^{>--}_{12}(t,0)G^{>--}_{22}(0,t)\rangle\\
={}& \tfrac{1}{2}[(\langle G^{>++}_{11}(t,0)G^{>++}_{21}(0,t)\rangle\\
&+ \langle G^{>++}_{21}(t,0)G^{>++}_{11}(0,t)\rangle)\\
&\times (\langle G^{>--}_{22}(t,0)G^{>--}_{12}(0,t)\rangle\\
&+ \langle G^{>--}_{12}(t,0)G^{>--}_{22}(0,t)\rangle)]\\
&+ \tfrac{1}{2}[(\langle G^{>++}_{11}(t,0)G^{>++}_{21}(0,t)\rangle\\
&- \langle G^{>++}_{21}(t,0)G^{>++}_{11}(0,t)\rangle)\\
&\times (\langle G^{>--}_{22}(t,0)G^{>--}_{12}(0,t)\rangle\\
&- \langle G^{>--}_{12}(t,0)G^{>--}_{22}(0,t)\rangle)]. \qquad \text{(A5)}
\end{aligned}$$

Each multiplier in the first term is equal to zero due to Eq. (22). From Eq. (7) one can get the following expression

$$\begin{aligned}
&\int d\Omega[\langle G^R_{11}(\Omega)\rangle\langle G^A_{12}(\Omega+\omega)\rangle - \langle G^R_{12}(\Omega)\rangle\langle G^A_{11}(\Omega+\omega)\rangle]\\
&\quad= \frac{-2T}{(\omega+2iQ)^2-4T^2} = \tilde{Z}_\omega. \qquad \text{(A6)}
\end{aligned}$$

Taking into account ladder diagrams (see Fig. 5) one can obtain a system of two linear equations

$$\begin{aligned}
\langle G^R_{11}G^A_{12}\rangle_\omega &= \Pi_{11}M^{12}_\omega + \Pi_{12}M^{22}_\omega,\\
\langle G^R_{12}G^A_{11}\rangle_\omega &= \Pi_{11}M^{11}_\omega + \Pi_{12}M^{21}_\omega, \qquad \text{(A7)}
\end{aligned}$$

where

$$\begin{aligned}
M^{12}_\omega &= \int d\Omega\langle G^R_{11}(\Omega)\rangle\langle G^A_{12}(\Omega+\omega)\rangle,\\
M^{11}_\omega &= \int d\Omega\langle G^R_{12}(\Omega)\rangle\langle G^A_{11}(\Omega+\omega)\rangle, \qquad \text{(A8)}
\end{aligned}$$

with the following relations being valid: $M^{11}_\omega = M^{22}_\omega$ and $M^{12}_\omega = M^{21}_\omega$. From Eqs. (A7)–(A8) follows

$$\begin{aligned}
Z_\omega &= \int d\Omega[\langle G^R_{11}(\Omega)G^A_{12}(\Omega+\omega)\rangle - \langle G^R_{12}(\Omega)G^A_{11}(\Omega+\omega)\rangle]\\
&= \tilde{Z}_\omega Y, \qquad \text{(A9)}
\end{aligned}$$

where Y is given by Eq. (14). Thus considering Eq. (A5) one can get

$$\frac{1}{2}\int d\omega_1 d\omega_2 Z_{\omega_1}Z_{\omega_2}e^{-\omega_1 t}e^{-i\omega_2 t} = -\frac{T^2}{Q^2}(e^{-\frac{2T^2 t}{Q}} - e^{-2Qt})^2. \qquad \text{(A10)}$$

Four similar terms in H and R [Eq. (A10)] reduce the multiplier 1/4. After performing all the calculations one can get a simple expression for $F_{\Psi_\pm}(t)$:

$$F_{\Psi_\pm} = \frac{1+x^2(t)}{2} \mp \frac{T^2}{Q^2}[e^{-\frac{2T^2 t}{Q}} - e^{-2Qt}]^2, \qquad \text{(A11)}$$

where $x(t) = (1+\frac{T^2}{Q^2})e^{-\frac{2T^2 t}{Q}} - \frac{T^2}{Q^2}e^{-2Qt}$.

APPENDIX B: TIME EVOLUTION OF TWO-QUBIT STATE $F_{\Phi_\pm}$

Let us now analyze another pair of Bell states

$$|\Phi_\pm(0)\rangle = \frac{|1\rangle_\sigma|1\rangle_{-\sigma} \pm |2\rangle_\sigma|2\rangle_{-\sigma}}{\sqrt{2}}, \tag{B1}$$

and calculate the probability $F_{\Psi_\pm}$.

$$\begin{aligned}F_{\Phi_\pm} = \tfrac{1}{4}\langle(&G_{11}^{>++}(t,0)G_{11}^{>--}(t,0) + G_{22}^{>++}(t,0)G_{22}^{>--}(t,0)\\ &\pm G_{12}^{>++}(t,0)G_{12}^{>--}(t,0) \pm G_{21}^{>++}(t,0)G_{21}^{>--}(t,0))\\ &\times (G_{11}^{>++}(0,t)G_{11}^{>--}(0,t) + G_{22}^{>++}(0,t)G_{22}^{>--}(0,t)\\ &\pm G_{12}^{>++}(0,t)G_{12}^{>--}(0,t) \pm G_{21}^{>++}(0,t)G_{21}^{>--}(0,t))\rangle,\end{aligned} \tag{B2}$$

as $\langle(G_{11}^{++}(t,0)G_{11}^{++}(0,t)\rangle = \langle(G_{11}^{++}(t,0)G_{11}^{--}(0,t)\rangle$ $\langle\xi_1^+\xi_1^-\rangle = \langle\xi_1^+\xi_1^+\rangle = \langle\xi_1^-\xi_1^-\rangle$. Using expressions (A2) and (A3) one can get

$$\begin{aligned}&\frac{1}{4}[2\langle G_{11}^{>++}(t,0)G_{11}^{>++}(0,t)\rangle\langle G_{11}^{>--}(t,0)G_{11}^{>--}(0,t)\rangle\\ &\quad + 2\langle G_{12}^{>++}(t,0)G_{21}^{>++}(0,t)\rangle\langle G_{12}^{>--}(t,0)G_{21}^{>--}(0,t)\rangle]\\ &= \frac{1+x^2(t)}{4},\end{aligned} \tag{B3}$$

where $x(t) = (1+\frac{T^2}{Q^2})e^{-\frac{2T^2t}{Q}} - \frac{T^2}{Q^2}e^{-2Qt}$. As $\langle\xi_1^\sigma\xi_2^{\sigma'}\rangle = 0$ for any σ,σ', $\langle G_{11}^R(t,0)G_{22}^A(0,t)\rangle = \langle G_{11}^R(t,0)\rangle\langle G_{22}^A(0,t)\rangle$ and $\langle G_{12}^R(t,0)G_{12}^A(0,t)\rangle = \langle G_{12}^R(t,0)\rangle\langle G_{12}^A(0,t)\rangle$. Taking into account Eqs. (7) and (26)

$$\begin{aligned}&\int d\omega_1 d\omega_2 \langle G_{11}^R G_{22}^A\rangle_{\omega_1}\langle G_{11}^R G_{22}^A\rangle_{\omega_2} e^{-i\omega_1 t}e^{-i\omega_2 t}\\ &= e^{-4Qt}\frac{(1+cos2Tt)^2}{4}.\end{aligned} \tag{B4}$$

Using Eq. (27) one can obtain

$$\begin{aligned}&\int d\omega_1 d\omega_2 \langle G_{12}^R G_{12}^A\rangle_{\omega_1}\langle G_{12}^R G_{12}^A\rangle_{\omega_2} e^{-i\omega_1 t}e^{-i\omega_2 t}\\ &= e^{-4Qt}\frac{(1-cos2Tt)^2}{4}.\end{aligned} \tag{B5}$$

The remaining terms have the same form as for the $|\Psi_\pm\rangle$ given by Eq. (A5)

$$H = \pm\frac{T^2}{Q^2}[e^{-\frac{2T^2t}{Q}} - e^{-2Qt}]^2. \tag{B6}$$

After performing all the calculations one can get a simple expression for $F_{\Phi_\pm}(t)$:

$$\begin{aligned}F_{\Phi_\pm} = \frac{1+x^2(t)}{4} + \frac{1+\cos^2(2Tt)}{4}e^{-4Qt}\\ \pm\frac{T^2}{Q^2}[e^{-\frac{2T^2t}{Q}} - e^{-2Qt}]^2.\end{aligned} \tag{B7}$$

For $T \ll Q$ oscillations are not present as the last term is of the order of T^2/Q^2 and up to the terms proportional to T^2/Q^2:

$$F_{\Phi_\pm} = \frac{1+e^{\frac{-4T^2t}{Q}}}{4} + \frac{1}{2}e^{-4Qt}. \tag{B8}$$

[1] T. F. Watson, S. G. J. Philips, E. Kawakami, D. R. Ward, P. Scarlino, M. Veldhorst, D. E. Savage, M. G. Lagally, M. Friesen, S. N. Coppersmith, M. A. Eriksson, and L. M. K. Vandersypen, A programmable two-qubit quantum processor in silicon, Nature (London) **555**, 633 (2018).

[2] C. H. Yang, R. C. C. Leon, J. C. C. Hwang, A. Saraiva, T. Tanttu, W. Huang, J. Camirand Lemyre, K. W. Chan, K. Y. Tan, F. E. Hudson, K. M. Itoh, A. Morello, M. Pioro-Ladriere, A. Laucht, and A. S. Dzurak, Operation of a silicon quantum processor unit cell above one Kelvin, Nature (London) **580**, 350 (2020).

[3] G. Burkard, Spin-entangled electrons in solid-state systems, J. Phys.: Condens. Matter **19**, 233202 (2007).

[4] D. P. DiVincenzo, The physical implementation of quantum computation, Fortschr. Phys. **48**, 771 (2000).

[5] K. De Greve, L. Yu, P. L. McMahon, J. S. Pelc, C. M. Natarajan, N. Y. Kim, E. Abe, S. Maier, C. Schneider, M. Kamp, S. Hofling, R. H. Hadfield, A. Forchel, M. M. Fejer, and Y. Yamamoto, Quantum-dot spin–photon entanglement via frequency downconversion to telecom wavelength, Nature (London) **491**, 421 (2012).

[6] W. B. Gao, P. Fallahi, E. Togan, J. Miguel-Sanchez, and A. Imamoglu, Observation of entanglement between a quantum dot spin and a single photon, Nature (London) **491**, 426 (2012).

[7] J. R. Schaibley, A. P. Burgers, G. A. McCracken, L.-M. Duan, P. R. Berman, D. G. Steel, A. S. Bracker, D. Gammon, and L. J. Sham, Demonstration of quantum entanglement between a single electron spin confined to an InAs quantum dot and a photon, Phys. Rev. Lett. **110**, 167401 (2013).

[8] C. H. Bennett, and S. J. Wiesner, Communication via one- and two-particle operators on Einstein-Podolsky-Rosen states, Phys. Rev. Lett. **69**, 2881 (1992).

[9] C. H. Bennett, and G. Brassard, in *Proceedings of the IEEE International Conference on Computers, Systems and Signal Processing*, Bangalore, India IEEE, New York (1984), p. 175.

[10] A. K. Ekert, Quantum cryptography based on Bell's theorem, Phys. Rev. Lett. **67**, 661 (1991).

[11] C. H. Bennett, G. Brassard, C. Crépeau, R. Jozsa, A. Peres, and W. K. Wootters, Teleporting an unknown quantum state via dual classical and Einstein-Podolsky-Rosen channels, Phys. Rev. Lett. **70**, 1895 (1993).

[12] D. Loss and D. P. DiVincenzo, Quantum computation with quantum dots, Phys. Rev. A **57**, 120 (1998).

[13] A. Imamoğlu, D. D. Awschalom, G. Burkard, D. P. DiVincenzo, D. Loss, M. Sherwin, and A. Small, Quantum information processing using quantum dot spins and cavity QED, Phys. Rev. Lett. **83**, 4204 (1999).

[14] W. Yao, R.-B. Liu, and L. J. Sham, Theory of control of the spin-photon interface for quantum networks, Phys. Rev. Lett. **95**, 030504 (2005).

[15] M. Blaauboer and D. P. DiVincenzo, Detecting entanglement using a double-quantum-dot turnstile, Phys. Rev. Lett. **95**, 160402 (2005).

[16] L. Robledo, J. Elzerman, G. Jundt, M. Atature, A. Hogele, S. Falt, and A. Imamoglu, Conditional dynamics of interacting quantum dots, Science **320**, 772 (2008).
[17] K. C. Nowack, M. Shafiei, M. Laforest, G. E. D. K. Prawiroatmodjo, L. R. Schreiber, C. Reichl, W. Wegscheider, and L. M. K. Vandersypen, Single-shot correlations and two-qubit gate of solid-state spins, Science **333**, 1269 (2011).
[18] M. D. Shulman, O. E. Dial, S. P. Harvey, H. Bluhm, V. Umansky, and A. Yakobi, Demonstration of entanglement of electrostatically coupled singlet-triplet qubits, Science **336**, 202 (2012).
[19] N. S. Maslova, P. I. Arseyev, and V. N. Mantsevich, Quenched dynamics of entangled states in correlated quantum dots, Phys. Rev. A **96**, 042301 (2017).
[20] G. E. Murgida, D. A. Wisniacki, and P. I. Tamborenea, Coherent control of interacting electrons in quantum dots via navigation in the energy spectrum, Phys. Rev. Lett. **99**, 036806 (2007).
[21] M. Kataoka, M. R. Astley, A. L. Thorn, D. K. L. Oi, C. H. W. Barnes, C. J. B. Ford, D. Anderson, G. A. C. Jones, I. Farrer, D. A. Ritchie, and M. Pepper, Coherent time evolution of a single-electron wave function, Phys. Rev. Lett. **102**, 156801 (2009).
[22] A. Putaja and E. Rasanen, Ultrafast sequential charge transfer in a double quantum dot, Phys. Rev. B **82**, 165336 (2010).
[23] L. Sælen, R. Nepstad, I. Degani, and J. P. Hansen, Optical control in coupled two-electron quantum dots, Phys. Rev. Lett. **100**, 046805 (2008).
[24] Y. P. Kandel, H. Qiao, S. Fallahi, G. C. Gardner, M. J. Manfra, and J. M. Nichol, Adiabatic quantum state transfer in a semiconductor quantum-dot spin chain, Nat. Commun. **12**, 2156 (2021).
[25] A. R. Mills, D. M. Zajac, M. J. Gullans, F. J. Schupp, T. M. Hazard, and J. R. Petta, Shuttling a single charge across a one-dimensional array of silicon quantum dots, Nat. Commun. **10**, 1063 (2019).
[26] U. Mukhopadhyay, J. P. Dehollan, C. Reichel, W. Wegscheider, and L. M. K. Vandersypen, A 2×2 quantum dot array with controllable inter-dot tunnel couplings, Appl. Phys. Lett. **112**, 183505 (2018).
[27] F.van Riggelen, N. W. Hendrickx, W. I. L. Lawrie, M. Russ, A. Sammak, G. Scappucci, and M. Veldhorst, A two-dimensional array of single-hole quantum dots, Appl. Phys. Lett. **118**, 044002 (2020).
[28] Y. Meir, N. S. Wingreen, and P. A. Lee, Low-temperature transport through a quantum dot: The Anderson model out of equilibrium, Phys. Rev. Lett. **70**, 2601 (1993).
[29] V. N. Mantsevich, and N. S. Maslova, Diferent behaviour of local tunneling conductivity for deep and shallow impurities due to Coulomb interaction, Solid State Commun. **150**, 2072 (2010).
[30] P. S. Cornaglia, and D. R. Grempel, Strongly correlated regimes in a double quantum dot device, Phys. Rev. B **71**, 075305 (2005).
[31] M. Y. Kagan, V. V. Val'kov, and S. V. Aksenov, Efects of anisotropy and Coulomb interactions on quantum transport in a quadruple quantum-dot structure, Phys. Rev. B **95**, 035411 (2017).
[32] V. N. Mantsevich, N. S. Maslova, and P. I. Arseyev, Charge trapping in the system of interacting quantum dots, Solid State Commun. **168**, 36 (2013).
[33] V. N. Mantsevich, N. S. Maslova, and P. I. Arseyev, Tunneling transport through multi-electrons states in coupled quantum dots with Coulomb correlations, Solid State Commun. **199**, 33 (2014).
[34] P. I. Arseyev, N. S. Masloava, and V. N. Mantsevich, Charge and spin configurations in the coupled quantum dots with Coulomb correlations induced by tunneling current, Eur. Phys. J. B **85**, 410 (2012).
[35] P. I. Arseyev, N. S. Masloava, and V. N. Mantsevich, Coulomb correlations effects on localized charge relaxation in the coupled quantum dots, Eur. Phys. J. B **85**, 249 (2012).
[36] I. Ozfidan, A. Trojnara, M. Korkusinski, and P. Hawrylak, Geometry, chirality, topology and electron–electron interactions in the quadruple quantum dot molecule, Solid State Commun. **172**, 15 (2013).
[37] I. P. Gimenez, C.-Y. Hsieh, M. Korkusinski, and P. Hawrylak, Charged-impurity-induced dephasing of a voltage-controlled coded qubit based on electron spin in a triple quantum dot, Phys. Rev. B **79**, 205311 (2009).
[38] V. Meden, and F. Marquardt, Correlation-induced resonances in transport through coupled quantum dots, Phys. Rev. Lett. **96**, 146801 (2006).
[39] P. I. Arseyev, N. S. Maslova, and V. N. Mantsevich, Correlation induced switching of the local spatial charge distribution in a two-level system, JETP Lett. **94**, 390 (2011).
[40] P. I. Arseev, N. S. Maslova, and V. N. Mantsevich, The effect of coulomb correlations on the nonequilibrium charge redistribution tuned by the tunneling current, J. Exp. Theor. Phys. **115**, 141 (2012).
[41] V. N. Mantsevich, and N. S. Maslova, Spatial effects of Fano resonance in local tunneling conductivity in the vicinity of impurity on semiconductor surface, JETP Lett. **91**, 139 (2010).
[42] K. Takeda, J. Kamioka, T. Otsuka, J. Yoneda, T. Nakajima, M. R. Delbecq, S. Amaha, G. Allison, T. Kodera, S. Oda, and S. Tarucha, A fault-tolerant addressable spin qubit in a natural silicon quantum dot, Sci. Adv. **2**, e1600694 (2016).
[43] J. Yoneda, K. Takeda, T. Otsuka, T. Nakajima, M. R. Delbecq, G. Allison, T. Honda, T. Kodera, S. Oda, Y. Hoshi, N. Usami, K. M. Itoh, and S. Tarucha, A quantum-dot spin qubit with coherence limited by charge noise and fidelity higher than 99.9% dot, Nat. Nanotechnol. **13**, 102 (2018).
[44] B. Paquelet Wuetz, D. D. Esposti, A.-M. J. Zwerver, S. V. Amitonov, M. Botifoll, J. Arbiol, A. Sammak, L. M. K. Vandersypen, M. Russ, and G. Scappucci, Reducing charge noise in quantum dots by using thin silicon quantum wells, Nat. Commun. **14**, 1385 (2023).
[45] K. D. Petersson, J. R. Petta, H. Lu, and A. C. Gossard, Quantum coherence in a one-electron semiconductor charge qubit, Phys. Rev. Lett. **105**, 246804 (2010).
[46] E. Dupont-Ferrier, B. Roche, B. Voisin, X. Jehl, R. Wacquez, M. Vinet, M. Sanquer, and S. D. Franceschi, Coherent coupling of two dopants in a silicon nanowire probed by Landau-Zener-Stückelberg interferometry, Phys. Rev. Lett. **110**, 136802 (2013).
[47] O. E. Dial, M. D. Shulman, S. P. Harvey, H. Bluhm, V. Umansky, and A. Yacoby, Charge noise spectroscopy using coherent exchange oscillations in a singlet-triplet qubit, Phys. Rev. Lett. **110**, 146804 (2013).

[48] E. Paladino, Y. M. Galperin, G. Falci, and B. L. Altshuler, 1/f noise: Implications for solid-state quantum information, Rev. Mod. Phys. **86**, 361 (2014).

[49] C. Müller, J. H. Cole, and J. Lisenfeld, Towards understanding two-level-systems in amorphous solids: Insights from quantum circuits, Rep. Prog. Phys. **82**, 124501 (2019).

[50] P. Dutta, Low-frequency fluctuations in solids: 1/f noise, Rev. Mod. Phys. **53**, 497 (1981).

[51] A. Bermeister, D. Keith, and D. Culcer, Charge noise, spin-orbit coupling, and dephasing of singlespin qubits, Appl. Phys. Lett. **105**, 192102 (2014).

[52] I. V. Krainov, A. P. Dmitriev, and N. S. Averkiev, Shot noise in resonant tunneling: Role of inelastic scattering, Phys. Rev. B **106**, 245421 (2022).

[53] J. R. Petta, A. C. Johnson, J. M. Taylor, E. A. Laird, A. Yacoby, M. D. Lukin, C. M. Marcus, M. P. Hanson, and A. C. Gossard, Coherent manipulation of coupled electron spins in semiconductor quantum dots, Science **309**, 2180 (2005).

[54] M. Veldhorst, C. H. Yang, J. C. C. Hwang, W. Huang, J. P. Dehollain, J. T. Muhonen, S. Simmons, A. Laucht, F. E. Hudson, K. M. Itoh, A. Morello, and A. S. Dzurak, A two-qubit logic gate in silicon, Nature (London) **526**, 410 (2015).

[55] M. Pioro-Ladriere, T. Obata, Y. Tokura, Y. S. Shin, T. Kubo, K. Yoshida, T. Taniyama, and S. Torucha, Electrically driven single-electron spin resonance in a slanting Zeeman field, Nat. Phys. **4**, 776 (2008).

[56] E. Kawakami, P. Scarlino, D. R. Ward, F. R. Braakman, D. E. Savage, M. G. Lagally, M. Friesen, S. N. Coppersmith, M. A. Eriksson, and L. M. K. Vandersypen, Electrical control of a long-lived spin qubit in a Si/SiGe quantum dot, Nat. Nanotechnol. **9**, 666 (2014).

[57] D. M. Zajac, A. J. Sigillito, M. Russ, F. Borjans, J. M. Taylor, G. Burkard, and J. R. Petta, Resonantly driven CNOT gate for electron spins, Science **359**, 439 (2018).

[58] R. C. C. Leon, C. H. Yang, J. C. C. Hwang, J. C. Lemyre, T. Tanttu, W. Huang, J. Y. Huang, F. E. Hudson, K. M. Itoh, A. Laucht, M. Pioro-Ladriere, A. Saraiva, and A. S. Dzurak, Bell-state tomography in a silicon many-electron artificial molecule, Nat. Commun. **12**, 3228 (2021).